

Co-implantation of Al⁺, P⁺, and S⁺ with Si⁺ implants into In_{0.53}Ga_{0.47}As

Aaron G. Lind, Henry L. Aldridge Jr., Kevin S. Jones, and Christopher Hatem

Citation: *Journal of Vacuum Science & Technology B* **33**, 051217 (2015); doi: 10.1116/1.4931030

View online: <http://dx.doi.org/10.1116/1.4931030>

View Table of Contents: <http://scitation.aip.org/content/avs/journal/jvstb/33/5?ver=pdfcov>

Published by the AVS: Science & Technology of Materials, Interfaces, and Processing

Articles you may be interested in

[Comparison of thermal annealing effects on electrical activation of MBE grown and ion implant Si-doped In_{0.53}Ga_{0.47}As](#)

J. Vac. Sci. Technol. B **33**, 021206 (2015); 10.1116/1.4914319

[Concentration-dependent diffusion of ion-implanted silicon in In_{0.53}Ga_{0.47}As](#)

Appl. Phys. Lett. **105**, 042113 (2014); 10.1063/1.4892079

[Electrical isolation of n- and p- In_{0.53}Ga_{0.47}As epilayers using ion irradiation](#)

J. Appl. Phys. **94**, 6616 (2003); 10.1063/1.1619567

[High concentration diffusivity and clustering of arsenic and phosphorus in silicon](#)


J. Appl. Phys. **83**, 2484 (1998); 10.1063/1.367008

[Implantation species dependence of transient enhanced diffusion in silicon](#)

J. Appl. Phys. **83**, 120 (1998); 10.1063/1.366708



Instruments for Advanced Science

<p>Contact Hiden Analytical for further details: W www.HidenAnalytical.com E info@hiden.co.uk</p> <p>CLICK TO VIEW our product catalogue</p>	 <p>Gas Analysis</p> <ul style="list-style-type: none"> › dynamic measurement of reaction gas streams › catalysis and thermal analysis › molecular beam studies › dissolved species probes › fermentation, environmental and ecological studies 	 <p>Surface Science</p> <ul style="list-style-type: none"> › UHV TPD › SIMS › end point detection in ion beam etch › elemental imaging - surface mapping 	 <p>Plasma Diagnostics</p> <ul style="list-style-type: none"> › plasma source characterization › etch and deposition process reaction › kinetic studies › analysis of neutral and radical species 	 <p>Vacuum Analysis</p> <ul style="list-style-type: none"> › partial pressure measurement and control of process gases › reactive sputter process control › vacuum diagnostics › vacuum coating process monitoring
---	--	--	--	--

Co-implantation of Al⁺, P⁺, and S⁺ with Si⁺ implants into In_{0.53}Ga_{0.47}As

Aaron G. Lind,^{a)} Henry L. Aldridge, Jr., and Kevin S. Jones

Department of Materials Science and Engineering, University of Florida, Gainesville, Florida 32611

Christopher Hatem

Applied Materials, Gloucester, Massachusetts 01930

(Received 14 July 2015; accepted 3 September 2015; published 16 September 2015)

Elevated temperature, nonamorphizing implants of Si⁺, and a second co-implant of either Al⁺, P⁺, or S⁺ at varying doses were performed into In_{0.53}Ga_{0.47}As to observe the effect that individual co-implant species had on the activation and diffusion of Si doping after postimplantation annealing. It was found that Al, P, and S co-implantation all resulted in a common activation limit of $1.7 \times 10^{19} \text{ cm}^{-3}$ for annealing treatments that resulted in Si profile motion. This is the same activation level observed for Si⁺ implants alone. The results of this work indicate that co-implantation of group V or VI species is an ineffective means for increasing donor activation of n-type dopants above $1.7 \times 10^{19} \text{ cm}^{-3}$ in InGaAs. The S⁺ co-implants did not show an additive effect in the total doping despite exhibiting significant activation when implanted alone. The observed n-type active carrier concentration limits appear to be the result of a crystalline thermodynamic limit rather than dopant specific limits. © 2015 American Vacuum Society.

[<http://dx.doi.org/10.1116/1.4931030>]

I. INTRODUCTION

Low active n-type carrier concentrations in III–V materials relative to those achievable in Si have long been recognized as one potential complicating factor for the adoption of III–V materials in CMOS devices. All future devices will require high doping concentrations in source/drain regions to achieve the low contact and access resistances required for efficient scaling. Both group IV and group VI dopants have been successfully implanted in InGaAs to create n-type regions, but most reports generally indicate that Si dopants exhibit the highest electrical activation in InGaAs.^{1,2} n-type doping concentrations on the order of $0.8\text{--}1.2 \times 10^{19} \text{ cm}^{-3}$ are regularly reported for Si implants into In_{0.53}Ga_{0.47}As, while epitaxial growth methods report electrically active Si concentrations higher than what has been achieved from ion implantation and annealing.^{1–7} Previous authors have hypothesized that the amphoteric nature of silicon leads to high levels of self-compensation from acceptor and donor creation as well as the formation of next nearest neighbor neutral pairs in III–V materials that are heavily doped with Si.^{8–10} In order to reduce Si self compensation, it has been further hypothesized that the introduction of excess group V species through ion implantation would help maintain stoichiometry of the implanted material by generating group III vacancies which would more readily allow Si occupation of group III sites upon implant activation.¹¹ Multiple studies of co-implantation with amphoteric dopants in III–V materials have been undertaken with varying outcomes.^{12–23} Many of these experiments either used very low doses of co-implants or used doses sufficient to amorphize the materials changing the as-implanted structure. The goal of this study was to use co-implant species with nearly the same mass as Si and elevated implant temperatures to avoid amorphization to determine the role of the co-implant species on Si activation in InGaAs.

^{a)}Electronic mail: aglind@ufl.edu

II. EXPERIMENT

Varying doses from 3×10^{13} to $6 \times 10^{14} \text{ cm}^{-2}$ of 20 keV Al⁺, P⁺ or S⁺ were implanted at 100 °C into 300 nm of metal-organic chemical vapor deposition grown undoped In_{0.53}Ga_{0.47}As on semi insulating InP substrates. The implant energies were chosen such that the implanted profiles of the co-implant species were coincident as predicted by the stopping range of ion in matter with the profile of the 20 keV, $6 \times 10^{14} \text{ cm}^{-2}$ Si⁺ implants used in this work. The varying dose Al⁺, P⁺, and S⁺ co-implants were performed first, followed by the constant 20 keV, $6 \times 10^{14} \text{ cm}^{-2}$ Si⁺ implantation. An implant temperature of 100 °C was chosen to prevent formation of an amorphous layer and prevention of amorphization was confirmed by cross-sectional transmission electron microscopy (TEM). The Al⁺ and P⁺ co-implants were chosen to study the chemical effect of group III and V implants while S⁺ co-implants were studied as to observe what effect an electrically active co-implant species would have on the maximum achievable carrier concentration. After implantation, all samples were coated with 15 nm of atomic layer deposition (ALD) Al₂O₃ deposited at 250 °C to protect against surface roughening during subsequent annealing treatments performed at 750 °C for either 5 s or 10 min to activate and diffuse the implanted dopants. After activation annealing, the dielectric cap was removed with buffered oxide etch (BOE) prior to van der Pauw Hall effect measurements of the active sheet number. Secondary ion mass spectroscopy (SIMS) using a 350 eV Cs⁺ beam was performed to monitor depth profiles of the implanted species after annealing.

III. RESULTS

Figure 1 shows SIMS of the postimplant Si concentration for the single 20 keV, $6 \times 10^{14} \text{ cm}^{-2}$ Si implant as well as the 20 keV, $6 \times 10^{14} \text{ cm}^{-2}$ P⁺, and Al⁺ co-implant Si⁺ profiles. From the postimplant SIMS profiles, it is evident that

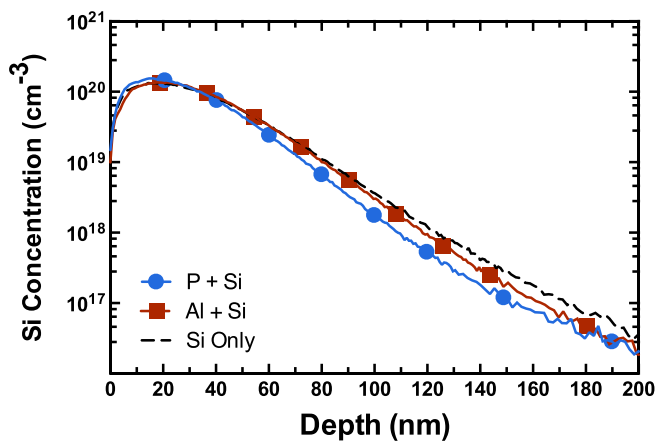


FIG. 1. (Color online) As implanted SIMS for a single 20 keV 6×10^{14} cm⁻² Si⁺ implant at 100 °C, as well as 20 keV 6×10^{14} cm⁻² Si⁺ implant co-implanted with 20 keV 6×10^{14} cm⁻² Al and P implants.

P⁺ implants result in slightly less random channeling in than Al⁺ implants and the Si⁺ implant alone is the deepest profile. The reduction in random channeling is likely the result of a slight increase in the nonamorphizing implant damage due to the co-implant and this damage is expected to increase with mass.

A. Carrier activation

The activation of 20 keV Si⁺ implanted In_{0.53}Ga_{0.47}As with varying doses of the Al⁺, P⁺, and S⁺ co-implant species after a 750 °C 5 s RTA is shown in Fig. 2(a) P⁺ co-implants do not result in any appreciable difference in activation with increasing co-implant dose while the Al⁺ co-implants are shown to initially decrease the active n-type carrier concentration with increasing co-implant dose. Active sheet number results from 10 m furnace anneal at 750 °C are shown in Fig. 2(b) and indicate that for extended anneal times there is no discernable difference in maximum carrier activation for Al⁺ or P⁺ co-implants. In the case of the 5 s RTA anneals, the maximum active sheet number was limited to approximately 1.5×10^{14} cm⁻² for P⁺ co-implants while longer 10 m

furnace anneals resulted in activation limited to 2×10^{14} cm⁻² for Si with or without a co-implant of Al⁺ or P⁺.

S⁺ was also used as co-implant species as S⁺ should also preferentially occupy group V sites and result in the creation of a shallow donor, leading to further an additional increase in the donor density. S⁺ co-implants exhibit similar activation limits to those of P⁺ co-implants despite S⁺ acting as a shallow donor in InGaAs when implanted without Si⁺. The active sheet number measurements for 750 °C 5 s RTA and 750 °C, 10 m furnace anneals for S⁺ co-implants shown in Figs. 2(a) and 2(b), respectively, are also shown to result in the same upper limit in activation that is observed with P⁺ co-implants alone. The common activation limit of S and P co-implants with Si seems especially surprising as S is an n-type dopant as well as being able to potentially contribute to a chemical co-implant effect by preferentially occupying the group V sublattice and causing Si to sit on the group III sublattice.

B. Si diffusion

Previous implant studies have concluded that Si redistribution upon annealing is minimal but more recent reports have indicated that Si redistribution is heavily concentration dependent above 2×10^{19} cm⁻³.^{2,24,25} The post 5 s RTA Si concentration profiles were measured by SIMS for the highest (6×10^{14} cm⁻²) and lowest (3×10^{13} cm⁻²) Al⁺ and P⁺ co-implant doses and are shown in Fig. 3(a). For the lowest dose P⁺ implant the characteristic shouldering of the heavily concentration dependent Si diffusion observed in previous studies is apparent but the effect is diminished for the higher dose P⁺ implant. In the case of Al⁺ co-implantation both the high and low dose co-implants result in minimal Si redistribution upon annealing. After a 10 m anneal, the Si concentration profile for the highest dose Al⁺, P⁺, and S⁺ implants is shown in Fig. 3(b). For longer anneal times, the behavior of Al, P, and S converge and result in similarly diffused Si profiles as shown in Fig. 3(b).

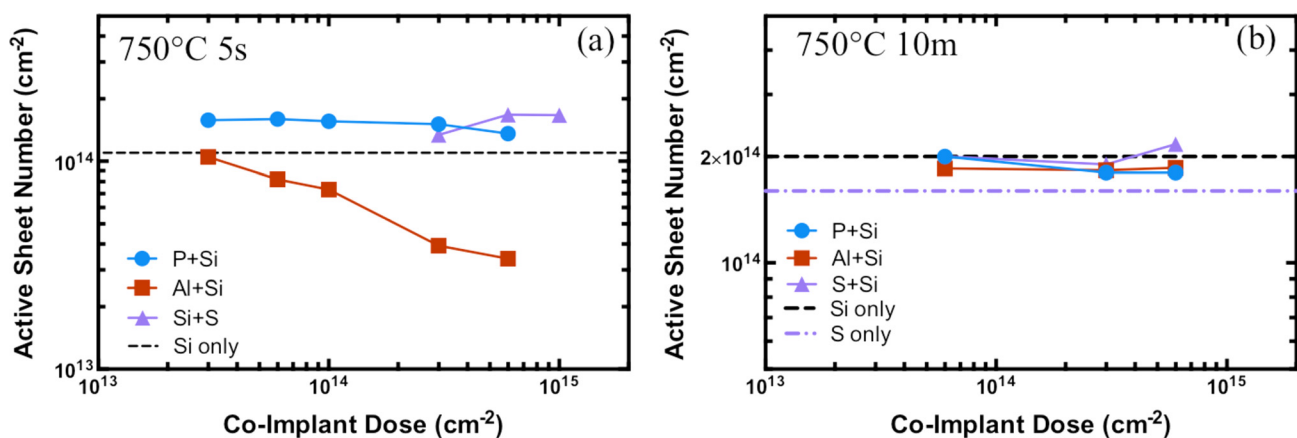


FIG. 2. (Color online) Postanneal active sheet number for 20 keV 6×10^{14} cm⁻² Si⁺ implant at 100 °C with varying co-implant doses of Al, P, and S after (a) 750 °C 5 s RTA and (b) 750 °C 10 m furnace anneal.

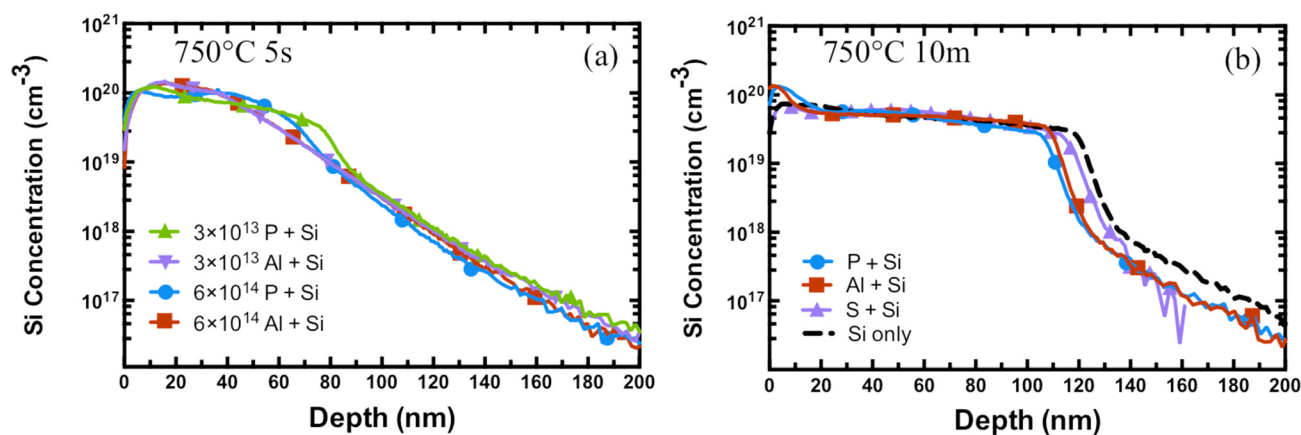


FIG. 3. (Color online) Postanneal Si concentration profiles for (a) 20 keV $6 \times 10^{14} \text{ cm}^{-2}$ Si⁺ implant at 100 °C with varying Al and P co-implant doses after a 750 °C 5 s RTA and for a (b) 20 keV $6 \times 10^{14} \text{ cm}^{-2}$ Si⁺ implants with 20 keV $6 \times 10^{14} \text{ cm}^{-2}$ Al, P, and S co-implants after a 750 °C 10 m furnace anneal.

C. Maximum active carrier concentrations

The results of the diffusion study echo those of the activation study as shorter duration anneals are shown to result in a larger difference in carrier activation and diffusion between Al⁺ and P⁺ co-implants whereas upon longer annealing times the differences in Si diffusion and activation with or without Al⁺ or P⁺ co-implants are shown to diminish. The active carrier concentration was calculated based on the post-anneal SIMS of Si and active sheet number by integrating under active carrier concentration limit such that the area under the Si profile up to the solubility limit was equal to the measured active sheet carrier concentration in order to form a more direct comparison of Si activation that accounts for Si diffusion effects. Using this method, it was found that for the Si implant co-implanted with $6 \times 10^{14} \text{ cm}^{-2}$ Al⁺, the active carrier concentration after a 5 s, 750 °C anneal was only $3 \times 10^{18} \text{ cm}^{-3}$ while the Si implanted sample with a $6 \times 10^{14} \text{ cm}^{-2}$ P⁺ co-implant resulted in activation of $1.6 \times 10^{19} \text{ cm}^{-3}$ equivalent to that observed in samples without a co-implant. Upon annealing at 750 °C for 10 min, the maximum carrier concentrations for the high dose and low dose Al⁺, P⁺, and S⁺ co-implants all converge to the same active carrier concentration of $1.7 \times 10^{19} \text{ cm}^{-3}$.

IV. DISCUSSION

Low activation of implanted n-type dopants relative to grown in dopants is commonly observed in III–V arsenides.^{1,3,26} For InGaAs, active implanted Si concentrations are generally limited to $1\text{--}2 \times 10^{19} \text{ cm}^{-3}$ but grown in Si concentrations as high as $6 \times 10^{19} \text{ cm}^{-3}$ have been reported in InGaAs.⁶ Previous authors have attributed the reduced activation of implanted Si to implant damage given the previous studies of proton irradiation and implants for isolation report that damage in these materials is p-type due to the introduction of trap states.^{27–29} Other authors have proposed that the reduced activation of implanted n and p-type dopants in III–V arsenides to reductions in chemical solubility due to a corresponding lack of group III or V elements required to maintain group III and group V site stoichiometry. Heckingbottom and Ambridge originally proposed the idea

of co-implantation of a group III or group V species as a means to preserve site stoichiometry with the corresponding introduction of either group II or group VI dopants.¹¹ Specifically, in the case of group VI dopants, it was proposed that the introduction of excess group III species would promote the creation of more group V vacancies to enhance group VI donor solubility.^{12,30–33} This same idea was applied to amphoteric dopant species with the thought that Si or Ge could be made more n-type in GaAs or InP by the implantation of As or P to promote creation of group III vacancies to increase occupation of group III sites with Si resulting in donors.^{13–16,18,20,21,34–36} The addition of group V species in the case of co-implantation with amphoteric dopants was also anticipated to reduce the propensity of group IV to occupy group V sites or the formation of IV–IV next nearest neighbor pairs and limit electrical activation.

In the case of p-type carbon implants in GaAs, the effectiveness of a co-implantation species was shown to be dependent on the atomic mass with inert co-implant species, which should not preferentially occupy lattice sites, resulting in increased p-type conductivity leading the authors to conclude that damage played a large role in the observed co-implant effect.^{19,37} Reports of group V co-implants with Ge and Si in GaAs and InP have generally shown increased electrical activation, but the improvements in activation are much less than the co-implant dose and are often observed for group IV implant doses which are not already heavily compensated and show high percent activation even without co-implantation. Banwell *et al.* showed the limited effectiveness of co-implants of As with Si in GaAs, but some co-implant results also report contradictory behavior to what is expected from a coimplant effect with Al co-implants also improving the n-type activation of Si in GaAs.^{13,22}

Previous studies generally evaluate the effectiveness of co-implants based on electrical activation, but direct evidence of site occupation is needed to confirm a chemical effect from co-implantation. Rutherford backscattering spectroscopy combined with particle induced x-ray emission (RBS/PIXE) has been used in the case of Si implants into

GaAs to examine the fraction of dopant sitting in interstitially or on lattice sites leading the authors to conclude that Si–Si next nearest pairs or Si_{As} caused the limited activation of Si; however, RBS/PIXE is not sensitive to the presence of Si-vacancy complexes that could also result in the observed compensation of dopants.^{8,38–40} Extended x-ray absorption fine structure (EXAFS) has been used successfully to study the effect of P co-implants on Ge site occupation in InP, but direct observation of lattice location of Si is made difficult in the InGaAs and GaAs system, given that the bond length difference in Si for Si–Ga or Si–As site is difficult to resolve using EXAFS.^{23,41,42} Optical methods have similar problems with resolution for the ternary systems, but Raman has had some success with identifying lattice site location of Si in binary III–V systems.^{43–46}

A. Al⁺, P⁺, and S⁺ co-implants

For short anneal times, there does appear to be some co-implant effect from the addition of Al⁺ co-implants to Si implanted InGaAs in that as the Al dose increases the active sheet number decreases as shown in Fig. 2(a). The post-anneal SIMS for the 750 °C 5 s RTA in Fig. 3(a) indicates that P⁺ implants result in more diffusion than Al⁺ implants for similar doses, but for longer anneal times, the Al⁺ and P⁺ implants show similar diffusion lengths. Si is thought to diffuse via a group III vacancy mechanism, and as a result, one interpretation of these diffusion results is that for short anneal times, the excess Al is competing with Si for group III lattice sites.^{10,47} The competition between Al and Si for lattice sites results in Si needing longer annealing times to find group III sublattice vacancies to move onto and the competition of Si with Al for group III site occupation results in reduced electrical activation of Si in InGaAs at short annealing times. At sufficiently high annealing times, the implanted Si and Al have both moved onto group III sublattices, and Si becomes active to the same upper limit of $1.7 \times 10^{19} \text{ cm}^{-3}$ with or without Al. For P⁺ implants, there is a limited competition for group V sites as Si prefers to occupy group III sites and Si is able to move onto group III lattice sites readily, but there is no evidence that P⁺ co-implantation promotes increased n-type activation of Si. In the case of P⁺ coimplants, there appears to be no co-implant effect in activation, but the SIMS of 750 °C 5 s RTA data suggests that higher dose P implants do impede Si diffusion at low times, suggesting that implant damage may be slowing Si diffusion. This interpretation is also supported in the comparison of the high dose Al and P co-implant diffusion with that of Si alone for the 10 m furnace anneals shown in Fig. 3(b). Both Al⁺ and P⁺ profiles are nearly coincident with the single Si⁺ implant showing slightly more diffusion. In this case, the resultant difference of diffusion may be from the excess interstitials resulting from the co-implants of Al and P relative to the single Si implant. If Si diffuses predominately through a vacancy mechanism, the interaction of Si-vacancy complex with excess interstitials could explain reduction in Si diffusion due to damage. The activation results of Si and S co-implantation indicate that the upper

active carrier concentration of these dopants in InGaAs is not the sum of their individual active concentrations. Despite S being an n-type dopant with activation levels of $5 \times 10^{18} \text{ cm}^{-3}$ the Si + S co-implants showed no appreciable difference in activation relative to Si alone for any of the annealing conditions studied.

B. Origins of n-type carrier saturation in InGaAs

One interpretation of the results of the co-implant experiments with Si and P which show no co-implant dose dependence on measured activation would be that in the case of co-implantation of Si and P, the increase in carriers resulting from co-implantation is perfectly matched by an opposing contribution from compensating damage since implant damage is shown to be compensating in InGaAs and GaAs. In the case of the Si + S, the enhancement in electrical activation from the S dopant and a corresponding co-implant effect would also be perfectly compensated by an increase in implant damage. Limited activation due to implant damage seems to be remarkably coincidental given that implant damage perfectly compensates both electrically active and isoelectronic co-implant species despite S and P having similar atomic masses. More recent studies also suggest that even heavily defective InGaAs result in similar n-type activation limits to InGaAs with significantly less damage, suggesting that damage is not a significant limitation for n-type activation in heavily doped substrates.⁴⁸

Ideally, co-implantation should promote Si occupation of group III sites but electrically there is no evidence that Si_{III} becomes preferred with increasing P co-implant dose. Without direct site evidence, it is impossible to say conclusively whether a co-implant effect is occurring in InGaAs, but the results of Si + P and Si + S implants do not behave as expected if amphoteric occupation by Si caused limited Si activation while S activation was limited due to a lack of group V sites to occupy. Since Si would be limited due to the amphoteric site occupation but S would not be limited by amphoteric site occupation, it might be reasonable to expect that the activation limit of these two dopants would be independent of one another. Instead, the results of Si + S co-implantation show that the active concentration is limited to same active level of Si alone, suggesting the presence of a common limiting mechanism for both Si and S.

The electrical results from Si + P and Si + S co-implants seem consistent with the amphoteric native defect model which predicts that the maximum n- or p-type solubility of dopants in a given semiconductor is largely an intrinsic material property and mediated by the formation of point defects.^{49–51} In the case of co-implantation in n-InGaAs, as the donor concentration increases, the energy to create compensating group V_{In} and V_{Ga} defects decreases and that these defects become more stable than Si_{III} or S_V defects. The large increase in cation vacancies are then capable of forming electrically compensated complexes with donor species. As a result, compensation by V_{III} in heavily doped materials will be dependent on the resulting Fermi level shift due to doping regardless of the dopant used. Fermi-level dependent

compensation is common to both n-type group IV dopants, which are amphoteric, and group VI dopants, which should overwhelmingly prefer to occupy through group V sublattice given the large formation energy of antisite defects. This is also evidenced by previous studies that show Si and Se implants have very similar maximum active concentration in InGaAs, despite Se being unable to self-compensate.^{1,2} Compensation behavior due to group III vacancy creation has been observed in Te and Si doped GaAs and InAs substrates grown from the liquid phase and the activation limits observed after annealing of implanted samples of InGaAs show similar activation behavior, suggesting the same mechanism is limiting in both ion implanted and growth doped materials.^{52–56} The defect limited explanation for n-type doping limits does not rule out the possibility of a co-implant effect, but it would explain why there would be limited evidence for it electrically since any net co-implant effect that causes increased n-type activation of Si would conceivably be neutralized by the formation of more compensating defects in InGaAs. Co-implants might be successful for increasing the donor solubility for Si doses with peak concentrations below the n-type activation limits in InGaAs, but these solubility limits can be readily reached with large doses of single Si implants following an optimized activating anneal.

The presence of vacancy defects is also likely evidenced by the highly concentration dependent nature of Si diffusion in these substrates.^{25,57} Silicon is believed to diffuse via a group III vacancy mechanism in InGaAs and GaAs and a large increase in the population of group III vacancies should enhance Si diffusion in InGaAs, as is observed at high doping concentrations. Previous studies of Si diffusion in InGaAs show that at high doping concentration above $2 \times 10^{19} \text{ cm}^{-3}$ where electrical activation is saturated, there is a significant amount of diffusion of Si despite Si being inactive at these concentrations, suggesting the presence of a mobile, yet electrically inactive Si_{III}-V_{III} complex. Positron annihilation spectroscopy studies also indicate that heavy n-type doping results in increasing concentration of vacancies in as-grown GaAs.^{58–61}

V. SUMMARY

Studies of co-implantation of Si with a group V or VI species have not been previously reported in InGaAs, but the results from this work indicate that n-type doping with Si and a group Al, P, or S co-implants tends to saturate to a maximum active carrier concentration of $\approx 1.7 \times 10^{19} \text{ cm}^{-3}$ for the implant conditions studied. The maximum activation occurring with co-implantation is no higher than the active carrier concentrations resulting from Si implantation alone, which is most consistent with the results obtained for Si implants into GaAs.¹³ Given the complications of directly observing how co-implant species affects site occupation, it is difficult to say based on the results of this study whether or not an actual co-implant effect is observed, but there is no evidence to suggest that co-implantation of group V or VI elements will result in increases of active carrier

concentration over what is readily achieved with Si alone. The results of this study suggest that even if co-implants were capable of controlling site stoichiometry that the resultant shift of Si onto group III sites and increase in n-type doping would likely be compensated by the production of Si-vacancy complexes.^{50,52,54,55,62,63} These vacancy defects also likely give rise to the heavily concentration dependent diffusion of Si in InGaAs and provide a much more succinct explanation for the common activation limit of Si and Si + S co-implants, as well as previous studies of amphoteric group IV dopants and group VI dopants in InGaAs which show similar maximum activation levels after implantation and annealing.^{1,2}

ACKNOWLEDGMENT

The authors acknowledge the Semiconductor Research Corporation for funding this work.

- ¹T. Penna, B. Tell, A. S. H. Liao, T. J. Bridges, and G. Burkhardt, *J. Appl. Phys.* **57**, 351 (1985).
- ²A. Alian *et al.*, *Microelectron. Eng.* **88**, 155 (2011).
- ³M. V. Rao, S. M. Gulwadi, P. E. Thompson, A. Fathimulla, and O. A. Aina, *JEM* **18**, 131 (1989).
- ⁴A. N. M. M. Choudhury, *Appl. Phys. Lett.* **40**, 607 (1982).
- ⁵Y. Fedoryshyn, M. Beck, P. Kaspar, and H. Jaeckel, *J. Appl. Phys.* **107**, 093710 (2010).
- ⁶T. Fujii, T. Inata, K. Ishii, and S. Hiyamizu, *Electron. Lett.* **22**, 191 (1986).
- ⁷R. A. Kubiak, J. J. Harris, and P. Dawson, *J. Appl. Phys.* **55**, 598 (1984).
- ⁸R. S. Bhattacharya, *Appl. Phys. Lett.* **40**, 890 (1982).
- ⁹J. Wagner, H. Seelewind, and W. Jantz, *J. Appl. Phys.* **67**, 1779 (1990).
- ¹⁰J. E. Northrup and S. B. Zhang, *Phys. Rev. B* **47**, 6791 (1993).
- ¹¹R. Heckingbottom and T. Ambridge, *Radiat. Eff.* **17**, 31 (1973).
- ¹²T. Ambridge, R. Heckingbottom, E. C. Bell, B. J. Sealy, K. G. Stephens, and R. K. E. L. Surridge, *Electron. Lett.* **11**, 314 (1975).
- ¹³T. C. Banwell, M. Mäenpää, M. A. Nicolet, and J. L. Tandon, *J. Phys. Chem. Solids* **44**, 507 (1982).
- ¹⁴A. R. Von Neida, S. J. Pearton, M. Stavola, and R. Caruso, *Appl. Phys. Lett.* **49**, 1708 (1986).
- ¹⁵F. Hyuga, H. Yamazaki, K. Watanabe, and J. Osaka, *Appl. Phys. Lett.* **50**, 1592 (1987).
- ¹⁶A. Dodabalapur and B. G. Streetman, *JEM* **18**, 65 (1989).
- ¹⁷H. Shen, G. Yang, Z. Zhou, and S. Zou, *Appl. Phys. Lett.* **56**, 463 (1990).
- ¹⁸S. Honglie, Y. Genqing, Z. Zuyao, and Z. Shichang, *Semicond. Sci. Technol.* **4**, 951 (1989).
- ¹⁹A. J. Moll, K. M. Yu, W. Walukiewicz, W. L. Hansen, and E. E. Haller, *Appl. Phys. Lett.* **60**, 2383 (1992).
- ²⁰P. Kringhøj, *Appl. Phys. Lett.* **64**, 351 (1994).
- ²¹J. C. Zolper and H. C. Chui, *Appl. Phys. Lett.* **68**, 3473 (1996).
- ²²J. P. de Souza and D. K. Sadana, *Appl. Phys. Lett.* **63**, 3200 (1993).
- ²³K. M. Yu and M. C. Ridgway, *Appl. Phys. Lett.* **71**, 939 (1997).
- ²⁴E. Hailemariam, S. J. Pearton, W. S. Hobson, H. S. Luftman, and A. P. Perley, *J. Appl. Phys.* **71**, 215 (1992).
- ²⁵H. L. Aldridge, A. G. Lind, M. E. Law, C. Hatem, and K. S. Jones, *Appl. Phys. Lett.* **105**, 042113 (2014).
- ²⁶A. G. Lind, N. G. Rudawski, N. J. Vito, C. Hatem, M. C. Ridgway, R. Hengstebeck, B. R. Yates, and K. S. Jones, *Appl. Phys. Lett.* **103**, 232102 (2013).
- ²⁷J. G. Williams, J. U. Patel, A. M. Ougouag, and S. Y. Yang, *J. Appl. Phys.* **70**, 4931 (1991).
- ²⁸H. J. Stein, *J. Appl. Phys.* **40**, 5300 (1969).
- ²⁹C. Carmody, H. H. Tan, and C. Jagadish, *J. Appl. Phys.* **94**, 6616 (2003).
- ³⁰E. B. Stoneham, G. A. Patterson, and J. M. Gladstone, *JEM* **9**, 371 (1979).
- ³¹M. V. Rao and R. K. Nadella, *J. Appl. Phys.* **67**, 1761 (1990).
- ³²S. Yamahata and S. Adachi, *Appl. Phys. Lett.* **52**, 1493 (1988).
- ³³D. E. Davies and P. J. McNally, *Appl. Phys. Lett.* **44**, 304 (1984).
- ³⁴N. N. Dymova, A. E. Kunitsyn, V. V. Chaldyshev, and A. V. Markov, *Semiconductors* **31**, 1217 (1997).
- ³⁵S. Sugitani, F. Hyuga, and K. Yamasaki, *J. Appl. Phys.* **67**, 552 (1990).
- ³⁶C. W. Farley, T. S. Kim, and B. G. Streetman, *JEM* **16**, 79 (1987).

- ³⁷A. J. Moll, J. W. Ager, K. M. Yu, W. Walukiewicz, and E. E. Haller, *J. Appl. Phys.* **74**, 7118 (1993).
- ³⁸R. S. Bhattacharya and P. P. Pronko, *Appl. Surf. Sci.* **18**, 1 (1984).
- ³⁹R. S. Bhattacharya, A. K. Rai, P. P. Pronoko, J. Narayan, S. C. Ling, and S. R. Wilson, *J. Phys. Chem. Solids* **44**, 61 (1983).
- ⁴⁰R. S. Bhattacharya, *Appl. Phys. Lett.* **42**, 880 (1983).
- ⁴¹K. M. Yu, A. J. Moll, W. Walukiewicz, N. Derhacopian, and C. Rossington, *Appl. Phys. Lett.* **64**, 1543 (1994).
- ⁴²S. Schuppler, D. L. Adler, L. N. Pfeiffer, K. W. West, E. E. Chaban, and P. H. Citrin, *Phys. Rev. B* **51**, 10527 (1995).
- ⁴³M. Uematsu, *J. Appl. Phys.* **69**, 1781 (1991).
- ⁴⁴M. Holtz, R. Zallen, A. E. Geissberger, and R. A. Sadler, *J. Appl. Phys.* **59**, 1946 (1986).
- ⁴⁵A. L. Alvarez, F. Calle, A. Sacedón, E. Calleja, E. Muñoz, J. Wagner, M. Maier, A. Mazuelas, and K. H. Ploog, *J. Appl. Phys.* **78**, 4690 (1995).
- ⁴⁶M. J. Ashwin *et al.*, *J. Appl. Phys.* **76**, 7839 (1994).
- ⁴⁷J. Dabrowski and J. E. Northrup, *Phys. Rev. B* **49**, 14286 (1994).
- ⁴⁸A. G. Lind, M. A. Gill, C. Hatem, and K. S. Jones, *Nucl. Instrum. Methods Phys. Res., B* **337**, 7 (2014).
- ⁴⁹W. Walukiewicz, *Phys. Rev. B* **50**, 5221 (1994).
- ⁵⁰W. Walukiewicz, *Appl. Phys. Lett.* **54**, 2094 (1989).
- ⁵¹W. Walukiewicz, *Phys. Rev. B* **37**, 4760 (1988).
- ⁵²T. Y. Tan, H. M. You, and U. M. Gosele, *Appl. Phys. A* **56**, 249 (1993).
- ⁵³D. Hurlle, *J. Phys. Chem. Solids* **40**, 627 (1979).
- ⁵⁴D. T. J. Hurle, *J. Appl. Phys.* **85**, 6957 (1999).
- ⁵⁵D. T. J. Hurle, *J. Appl. Phys.* **107**, 121301 (2010).
- ⁵⁶D. Hurlle, *J. Phys. Chem. Solids* **40**, 639 (1979).
- ⁵⁷A. G. Lind, H. L. Aldridge, Jr., C. C. Bomberger, C. Hatem, J. M. O. Zide, and K. S. Jones, *J. Vac. Sci. Technol. B* **33**, 021206 (2015).
- ⁵⁸J. Gebauer, R. Krause-Rehberg, C. Domke, P. Ebert, and K. Urban, *Phys. Rev. Lett.* **78**, 3334 (1997).
- ⁵⁹J.-L. Lee, L. Wei, S. Tanigawa, and M. Kawabe, *J. Appl. Phys.* **68**, 5571 (1990).
- ⁶⁰J.-L. Lee, A. Uedono, S. Tanigawa, and J. Y. Lee, *J. Appl. Phys.* **67**, 6153 (1990).
- ⁶¹J.-L. Lee, L. Wei, S. Tanigawa, and M. Kawabe, *Appl. Phys. Lett.* **58**, 1524 (1991).
- ⁶²W. Walukiewicz, *Phys. B: Condens. Matter* **302**, 123 (2001).
- ⁶³S. B. Zhang, S.-H. Wei, and A. Zunger, *Phys. B: Condens. Matter* **273**, 976 (1999).